External Reflection FTIR of Peptide Monolayer Films in Situ at the Air/Water Interface: Experimental Design, Spectra-Structure Correlations, and Effects of Hydrogen-Deuterium Exchange

Carol R. Flach,* Joseph W. Brauner,* John W. Taylor,‡ Randall C. Baldwin,‡ and Richard Mendelsohn*
*Departments of Chemistry, Newark College of Arts and Science, Rutgers University, 73 Warren Street, Newark, New Jersey 07102, and ‡Wright-Riemann Labs, Busch Campus, Rutgers University, Piscataway, New Jersey 08903

ABSTRACT A Fourier transform infrared spectrometer has been interfaced with a surface balance and a new external reflection infrared sampling accessory, which permits the acquisition of spectra from protein monolayers in situ at the air/water interface. The accessory, a sample shuttle that permits the collection of spectra in alternating fashion from sample and background troughs, reduces interference from water vapor rotation-vibration bands in the amide I and amide II regions of protein spectra (1520–1690 cm^{-1}) by nearly an order of magnitude. Residual interference from water vapor absorbance ranges from 50 to 200 microabsorbance units. The performance of the device is demonstrated through spectra of synthetic peptides designed to adopt α-helical, antiparallel β-sheet, mixed β-sheet/β-turn, and unordered conformations at the air/water interface. The extent of exchange on the surface can be monitored from the relative intensities of the amide II and amide I modes. Hydrogen-deuterium exchange may lower the amide I frequency by as much as 11–12 cm^{-1} for helical secondary structures. This shifts the vibrational mode into a region normally associated with unordered structures and leads to uncertainties in the application of algorithms commonly used for determination of secondary structure from amide I contours of proteins in D_2O solution.

INTRODUCTION

Insoluble monolayers at the air/water (A/W) interface provide models for a wide variety of biological systems, thereby permitting fundamental investigations of molecular aggregation, orientation, and domain formation in biomembranes. Although the need for the acquisition of molecular structure information from these systems was evident at an early stage, technological difficulties were such that, until a few years ago, the prime means of monolayer characterization came from the techniques of surface chemistry, generally through the construction of surface pressure (π)/area isotherms. Although these provide a thorough characterization of surface thermodynamics, accurate molecular structure inferences are difficult to draw from such data.

Recent years have seen the development of several techniques for molecular characterization of monolayer film properties. Epifluorescence microscopy, elaborated in the area of phospholipid membrane models by McConnell and others, has led to an understanding of domain structure at the A/W interface and its relationship to thermodynamic quantities (von Tscharner and McConnell, 1981; Peters and Beck, 1983; McConnell et al., 1984). Möhwald and his co-workers have used x-ray scattering to determine acyl chain orientation in lipid films (Möhwald, 1990; Helm et al., 1991; Böhm et al., 1993).

The techniques of vibrational spectroscopy are particularly well suited for the acquisition of molecular structure information. Infrared (IR) and Raman spectroscopies do not require probe molecules, which may perturb monolayer properties, and benefit from the availability of an extensive body of spectra-structure correlations from bulk-phase measurements. The prime drawback of these methods is the weakness of the spectral signals from monolayers.

The feasibility of acquiring external reflectance FTIR (IRRAS) spectra from phospholipid monolayer films at the A/W interface under conditions of controlled π was first demonstrated in a series of elegant experiments by Dluhy and coworkers, who observed a π-induced phase transition in films of 1,2- dipalmitoylphosphatidylcholine (Dluhy, 1986; Dluhy et al., 1988; Mitchell and Dluhy, 1988). Extensions of the work in a collaborative effort between Dluhy's lab and this one have involved the examination of bovine lung surfactant (Dluhy et al., 1989). Recently we have demonstrated the exclusion of particular components from mixed monolayer films at high πs (Pastrana-Rios et al., 1994).

The logical next step in the application of in situ IRRAS at the A/W interface to the study of membrane organization and related problems requires the acquisition of spectra from protein monolayer films. The technical problem is the elimination of interference from water vapor rotation-vibration bands that absorb strongly in the region of the IR spectra of proteins that is most sensitive to secondary structure, namely the amide I and II spectral regions (1520–1690 cm^{-1}). In the current paper, we describe an accessory for a coupled FTIR/surface balance apparatus that permits the acquisition of protein monolayer spectra in situ at the A/W interface. A preliminary communication describing an early version of the apparatus has appeared (Flach et al., 1993a).

The scientific issue selected to demonstrate the utility of the device is the determination of the secondary structure of

Received for publication 19 January 1994 and in final form 5 April 1994.

Address reprint requests to Richard Mendelsohn, Department of Chemistry, Olson Laboratories; Room 304, Rutgers University, 73 Warren Street, Newark, NJ 01702. Tel.:201-648-5613; Fax: 201-648-1264.

Abbreviations used: π, surface pressure; IRRAS, infrared reflection absorption spectroscopy (spectra); ATR, attenuated total reflectance; CD, circular dichroism; mAU, milliabsorbance units.

0006-3495/94/07/402/09 $2.00

several synthetic surface-active peptides spread as monolayers at the A/W interface. Methods currently used for this determination are limited to circular dichroism (CD) or attenuated total reflectance (ATR)-IR studies of films that have been transferred to quartz slides (Cornell, 1978; DeGrado and Lear, 1985; Taylor, 1990) and curve fitting of pressure-area isotherms to equations of state (Fukushima et al, 1979; DeGrado and Lear, 1985; Taylor, 1990). The reliability of these methods is untested. In addition, the substantial effects of hydrogen-deuterium (HD) exchange on the amide I frequency have been cataloged. The results call into question some current procedures for the determination of protein secondary structure in D_2O solutions.

MATERIALS AND METHODS

Protein isolation and peptide synthesis

Hydrophobic lung surfactant protein, SP-C, was isolated from bovine lung lavage and characterized as described previously (Pastrana et al., 1991). Other peptides, designated as I through IV (Fig. 1) were designed to achieve specific amphiphilic conformations at the A/W interface. Peptide I was a gift from E.T. Kaiser (Osterman and Kaiser, 1985). Peptide III (Taylor, 1990) and peptide IV (Ösapay and Taylor, 1992) were synthesized and characterized as described previously. Peptide II was synthesized by standard solid-phase synthesis methods (Barany and Merrifield, 1979), employing N_α-Boc protection and a symmetric anhydride coupling protocol. After HF cleavage and deprotection, the crude peptide was purified to homogeneity by reversed-phase high-performance liquid chromotography and characterized by amino acid analysis.

The putative conformations assigned to peptides I-IV at the A/W interface are indicated in Table 1. Monolayers of peptides I and III are assigned the β-sheet and α-helical conformations, respectively, on the basis of their CD spectra after transfer onto quartz slides and the shapes of their compression isotherms, as described previously (Taylor, 1990). A sheet-turn conformation was designated for peptide II on the basis of both its design and the characteristics of its monolayers at the A/W interface. This peptide was designed to form amphiphilic β-sheet structures through the formation of four short (three residue) amphiphilic β-strands linked by three β-turns centered around the Pro-Asp sequences in its structure. Curve-fitting analyses of the isotherms obtained upon compression of the peptide II monolayers indicate a low limiting area, low compressibility, and a high level of aggregation (R.C. Baldwin, G. Shuiyun, and J.W. Taylor, unpublished results). This is consistent with the formation of a β-sheet structure (DeGrado and Lear, 1985; Taylor, 1990). Peptide IV was designated as having an unordered conformation at the A/W interface on the basis of its limiting surface area of 37 Å^2/residue (G. Ösapay and J.W. Taylor, unpublished results). This compares to a corresponding value of 23 Å^2/residue for peptide III. However, CD spectra obtained from transferred peptide IV monolayers on quartz slides indicated a mixture of helical and unordered conformations (Ösapay and Taylor, 1992).

Peptide I: H-Val-Glu-Val-Orn(TFA)-Val^5-Glu-Val-Orn(TFA)-Val-Glu^{10}-Val-Orn(TFA)-Val-OH

Peptide II: Ac-(Asp-Ile-Arg-Phe-Pro)$_4$-NH_2

Peptide III: H-Pro-Lys-Leu-Glu-Glu^5-Leu-Lys-Glu-Lys-Leu^{10}-Lys-Glu-Leu-Leu-Glu^{15}-Lys-Leu-Lys-Glu-Lys^{20}-Leu-Ala-OH

Peptide IV: H-(Lys-Leu-Lys(Ac)-Glu-Leu-Lys-Gln)$_3$-OH

FIGURE 1 Amino acid sequences of peptides used in the current work. Peptide I contains N^δ-trifluoroacetyl-L-ornithine residues, abbreviated as Orn(TFA). Peptide IV contains an N^ε-acetyl-L-lysine residue, abbreviated as Lys(Ac).

TABLE 1 Amide I and I′ band IRRAS observed frequencies

Peptides	Buffered subphase	
	H_2O	D_2O
	(cm^{-1})	
Peptide I (β-sheet)[a]	1627	1689/1620
Peptide II (β-sheet/β-turn)[a]	1636	1627
Peptide III (α-helix)[a]	1656	1645
Peptide IV (unordered)[a]	1655	1642

[a] Putative conformations assigned before the current study. See text for details.

Surface films

The lung surfactant protein, SP-C, was dissolved in a $CHCl_3$/MeOH 3:2 (v/v) solution (~50 μg/ml). Peptide samples were prepared by dissolving approximately 0.15 mg of peptide in 1 ml 1 mM HCl in 0.15 M NaCl/H_2O (double distilled) or in 1 ml 1 mM DCl in 0.15 M NaCl/D_2O. The surface balance, described elsewhere (Boyle and Mautone, 1982; Flach et al., 1993a), consisted of a modified dual well Teflon trough (Fig. 2), a 150-mesh stainless steel screen, and a roughened Pt plate. All were cleaned before use by soaking in a chromic acid solution (Chromerge, Fisher Scientific, Fairlawn, NJ). The subphase consisted of a Tris buffer (10 mM Tris, 50 mM NaCl) in H_2O, pH~7.4 or in D_2O, pD~7.4. Monolayers were spread from protein or peptide solutions by touching drops from the tip of a long-needle 50-μl syringe to the surface, while increasing the surface area to its maximum (~90 cm^2) by raising the screen. Sufficient time (5–10 min) was allowed for film equilibration and/or solvent evaporation before film compression. Films were compressed by lowering the screen to obtain preset surface tension values, and then the IRRAS spectra were acquired.

IRRAS with water vapor compensation modification

The original design of the miniaturized surface balance/IR spectrometer used in this study has been described elsewhere (Flach et al., 1993a). In the

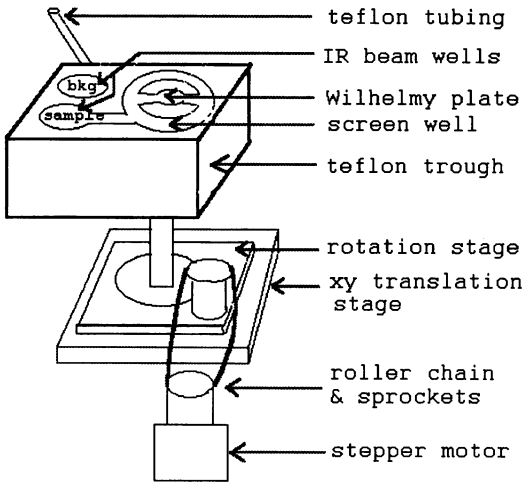

FIGURE 2 Schematic drawing of the trough-water vapor compensation module. Approximate dimensions of the Teflon trough are 11.5 × 7 × 4 cm^3 (L × W × H). The diameter of the sample and background wells is 2.5 cm, and they are 0.6 cm deep. The diameter of the screen well is 5.1 cm, and it is 2.9 cm deep. The dimensions of the channel connecting the sample well and screen well are 3 × 0.8 × 0.4 cm^3 (L × W × D). The diameter of the well for the Wilhelmy plate is 1.7 cm, and it is 0.6 cm deep.

current work, the device has been modified to reduce water vapor rotation-vibration peaks for the purpose of obtaining protein secondary structure information from the amide I spectral region (1600–1700 cm^{-1}). The miniaturized trough (volume ~40 ml) makes practical the use of a D_2O subphase. This in turn eliminates the distorting effects of the strong H_2O absorption band centered at 1643 cm^{-1} and decreases the magnitude of the water vapor bands in this region, but it increases the magnitude of the HDO bands. Even under conditions of rapid purge, water vapor, and HDO bands of varying magnitude remain. These hamper detection in the amide I (or I') region, which, for a monolayer, is often less than 2 milliabsorbance units (mAU).

A shuttle system, shown in Fig. 2, was designed to reduce the intensity of water vapor bands by alternating the collection of scans between background and sample wells over a small time interval through rotation of the trough. The trough is mounted to a rotation stage (Newport Corp., Irvine, CA) that is driven by a computer-controlled stepping motor (Alpha Products, Fairfield, CT). The motion of the stepping motor shaft is translated to the trough via a roller chain and sprockets (Small Parts, Inc., Miami Lakes, FL) that connect the motor shaft to a shaft that turns the rotation stage. The stepper motor is activated and controlled using commands sent through the computer printer port. The well for the Wilhelmy plate lies on the axis of rotation, thereby minimizing the disturbance to the surface film upon rotation. The sample and background wells are connected underneath by a drilled channel to minimize the difference in the IR beam path length through equalization of the level of the subphase in both wells. The exterior optical system and surface balance are enclosed in a plexiglass chamber to exclude contaminants and to permit purging. Typically, the spectrometer and plexiglass chamber are purged before spectra are acquired, with dry air overnight when a D_2O subphase is used, and for a few hours when an H_2O subphase is used. A solvent delivery system consisting of Teflon tubing connecting the sample and background well channels to a three-way valve and a 20-ml syringe outside the plexiglass enclosure permits replenishment of the subphase without breaking the purge. Occasionally, a film of decanol was spread from a $CHCl_3$/MeOH (3:2 v/v) solution on the background well to inhibit subphase evaporation and to create a meniscus shape similar to that of a peptide film on the sample well.

The spectrometer used was a Bio-Rad (Digilab, Cambridge, MA) FTS 40A, equipped with an external narrow band Mercury-Cadmium-Telluride detector. Interferograms were collected at 4 cm^{-1} spectral resolution at an angle of incidence centered at 45° (beam spread ± 4°), apodized with a triangular function and Fourier transformed with one level of zero-filling to yield spectral data encoded at ~2-cm^{-1} intervals. The sample and reference wells are aligned in the IR beam in alternating fashion. The Bio-Rad 3200 Data Station permits successive coaddition of scans to preexisting interferogram files. Typically, a total of 128 scans are coadded in 2 cycles of 64 scans each, where each cycle consisted of sampling 64 scans from the background and then from the sample well. A delay time of 20 s between trough rotation and data acquisition was found to be necessary to reestablish the surface equilibrium. The IRRAS spectra are plotted as $-\log(R/R_0)$, where R is the single-beam reflectance of a monolayer covered surface, and R_0 is the single-beam reflectance of the subphase. Negative peaks are observed, as anticipated at this angle of incidence from the three-layer Fresnel equations using the appropriate optical constants (McIntyre, 1973; Dluhy, 1986). Baselines were flattened and residual water vapor bands were subtracted using an appropriate reference spectrum with manufacturer-supplied software. For determination of the frequency positions and bandwidths at half-height of the amide I and II bands, spectra were Fourier smoothed using a breakpoint of 0.80. Data manipulations were accomplished off-line on a minicomputer with software written at the National Research Council of Canada.

ATR FTIR

ATR-IR spectra of dried peptide films were acquired on a Research Series (RS-1) spectrophotometer (Mattson Instruments Inc., Madison, WI) equipped with an MCT detector and a Spectra-Tech, Inc. (Stamford, CT) Out-of-Compartment model ATR accessory with a ZnSe crystal for ATR. Films were dried on the crystal by applying microliter quantities of peptide solution and allowing time for solvent evaporation at 45°C. The sample temperature for IR measurements was 37°C. Interferograms were collected at 4-cm^{-1} resolution, apodized with a triangular function, and Fourier transformed with one level of zero-filling to yield spectral data encoded at 2-cm^{-1} intervals. Appropriate reference spectra were subtracted using manufacturer-supplied software.

Circular Dichroism Spectroscopy

Circular dichroism (CD) spectra of peptide solutions, were recorded on an Instruments, SA (distributed by SPEX Industries, Metuchen, NJ) JY Mark 6 spectrometer. Reference spectra were subtracted using manufacturer-supplied software.

Spectral simulations

To facilitate the interpretation of the observed IRRAS of peptide monolayer films on H_2O and D_2O, the exact equations of McIntyre (1973) giving the reflectance of a three-layer system were programmed. The computed reflectance absorbance is given by

$$A = -\log(R_{123}/R_{13}),$$

where R_{13} is the reflectance of the A/W interface and R_{123} is the reflectance of the air/film/water system. The reflectance, R, is the square of the absolute value of the corresponding reflection coefficients, for example,

$$R_{13} = |r_{13}|^2.$$

These reflection coefficients are given by Eqs. (12a), (12b), and (16) in McIntyre's paper.

The film was not taken as isotropic, but rather, three Cartesian components for the index of refraction, n, and the extinction coefficient, k, were calculated according to Fraser's equations for fiber orientation (Fraser and MacRae, 1973). That is, the extinction coefficient of the film is taken as the product of an amplitude factor and an orientational factor,

$$k_{2\text{eff}} = k_{2\text{amp}} \cdot k_{2\text{orient}}.$$

For parallel polarization,

$$k_{2\text{orient}} = (k_{2x} \cdot \cos^2\phi) + (k_{2z} \cdot \sin^2\phi),$$

where ϕ is the angle of incidence.

For perpendicular polarization,

$$k_{2\text{orient}} = k_{2y},$$

where

$$k_{2x} = k_{2y} = \{(f \cdot \sin^2\alpha)/2\} + \{(1 - f)/3\}.$$

$$k_{2z} = (f \cdot \cos^2\alpha) + \{(1-f)/3\},$$

where α is the angle between the chain axis and the transition dipole and f is the order parameter described by

$$f = \{(3 \cdot \cos^2\theta) - 1\}/2. \qquad \theta = \text{tilt angle from bilayer normal.}$$

The amplitude part of the film extinction coefficient was taken as

$$k_{2\text{amp}} = (k_{\max} \cdot \gamma^2)/(4\mu^2 + \gamma^2),$$

where γ is proportional to the full width at half-height of the Lorentzian describing the film's absorption band, μ is the displacement from the center frequency of the band, and $k_{\max}$ is the absorbance at the band center.

The index of refraction for the film (Becker, 1964) was taken as

$$n_2 = 1.35 - (2\mu \cdot k_{\max} \cdot \gamma \cdot k_{2\text{orient}})/(4\mu^2 + \gamma^2).$$

The n and k values for the H_2O substrate were those of Downing and Williams (1975) interpolated to a 1-cm^{-1} interval. The n and k values for D_2O in the range 1600–1700 cm^{-1} were assumed to equal those of H_2O in the range 2200–2300 cm^{-1}, as the combination band of D_2O in this region (1600–1700 cm^{-1}) is similar in shape and amplitude to that of H_2O in the 2200–2300-cm^{-1} region.

Simulations for the parallel and perpendicular components of an IRRAS band of a Lorentzian centered at 1656 cm^{-1} on H_2O and D_2O substrates are shown in Fig. 3, *A* and *B*, respectively. The difference in the reflectance-absorbance between the two polarizations is striking, with the parallel component about an order of magnitude more intense than the perpendicular. The simulations also reveal that the band on a water substrate is much more distorted than the corresponding band from a D_2O substrate. The maximum on H_2O in the parallel component is shifted ~2 cm^{-1} up in frequency when compared to the Lorentzian and is shifted up less than 1 cm^{-1} for the perpendicular component. The band for the parallel component on H_2O is narrower than the original Lorentzian. For a D_2O subphase, the maximum in the parallel component is shifted down ~1 cm^{-1} with no shift in the perpendicular component and little change in the apparent linewidth.

The baseline for the simulated IRRAS does not extrapolate to zero, because the refractive index of the film (n_2) continues to modify the reflectance, even though the extinction coefficient (k_2) is vanishingly small. The three-layer reflectance is never the same as the two-layer reflectance.

RESULTS

Spectral improvement due to H_2O vapor compensation

Fig. 4 displays the amide I and II regions (1500–1700 cm^{-1}) of the IRRAS for the hydrophobic lung surfactant protein, SP-C, on a D_2O subphase before and after implementation of the shuttle modification. Significant improvement is noted in the quality of the spectra in this region as the intensity of the main sharp water vapor bands is decreased by a factor of ~7.5 from ~1.5 to ~0.2 mAU between Fig. 4, *A* and *B*, respectively. Reduced interference from water vapor permits the location of peaks and the integration of band intensities for amide I and II, thereby permitting the determination of secondary structure and the acquisition of HD exchange information. The structural information from these data is discussed later in the text.

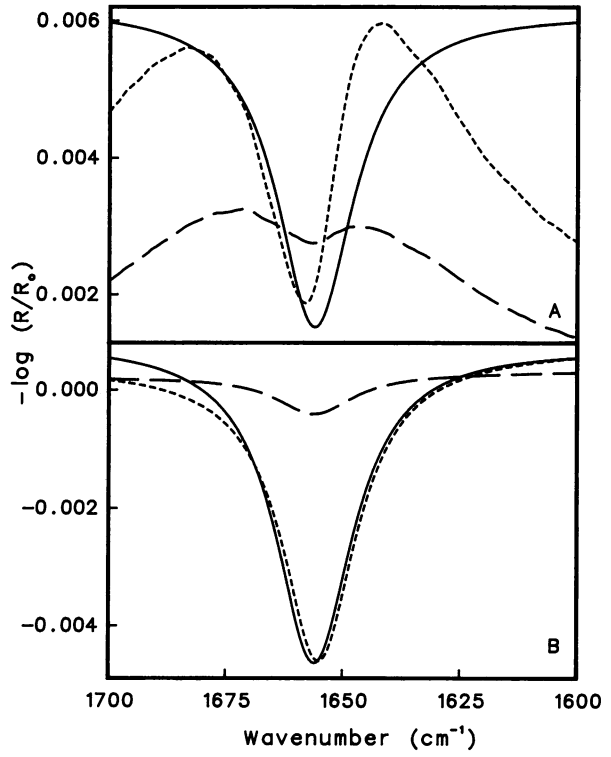

FIGURE 3 Spectral simulations for the parallel and perpendicular amplitudes of amide I IRRAS bands from (*A*) an H_2O subphase and (*B*) a D_2O subphase. The solid line represents k, the extinction coefficient, assumed to have a Lorentzian lineshape; (- - - -) represents the parallel component; and (— —) represents the perpendicular component of the calculated IRRAS band. Assumed values: angle of incidence = 45°; tilt angle of helix axis with normal to surface = 10°; length of helix axis = 50 Å; angle between helix axis and amide I transition dipole = 28°; ν_{max} = 1656 cm^{-1}; absorbance at ν_{max} = 0.25 AU; and full width at half-height = 20 cm^{-1}.

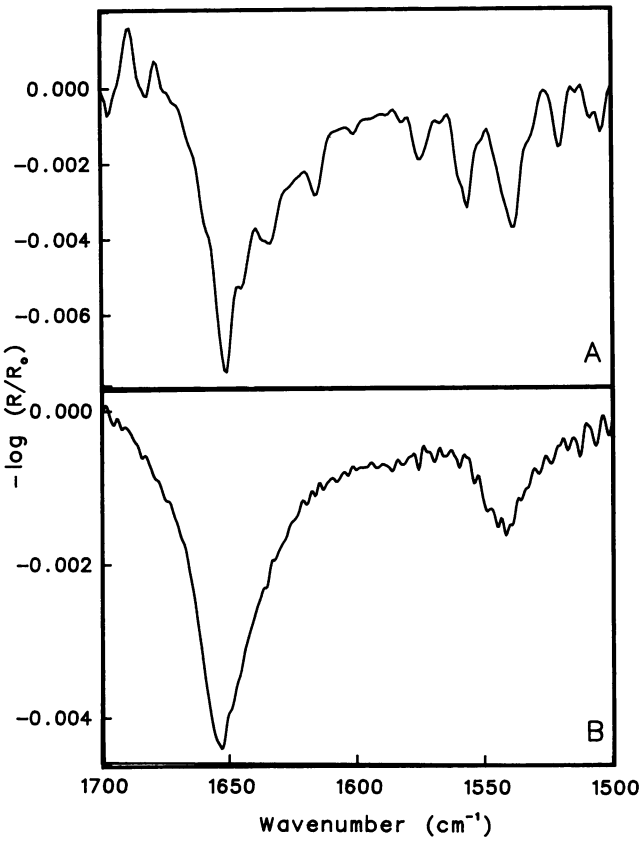

FIGURE 4 The IRRAS of the amide I and II regions for a monolayer film of the surfactant protein, SP-C, on a D_2O subphase before (*A*) and after (*B*) the implementation of the water vapor compensation unit. Water vapor has been subtracted from (*A*) 2048 scans, but not from (*B*) 1024 scans. Both spectra were acquired at $\pi \approx$ 15–20 dyne/cm and were baseline corrected. Water vapor distortion in (*A*) may account for the majority of the additional intensity observed in the amide I band (~1654 cm^{-1}) when compared to (*B*).

Peptides I and II (putative β-sheet and mixed sheet-turn structures) at the A/W interface

Fig. 5 *A* displays the IRRAS of the amide I and II regions for monolayer films of peptide I (putative β-sheet peptide film) at the air/H_2O and air/D_2O interfaces. In Fig. 5 *B* the same spectra are displayed after smoothing with a breakpoint of 0.80 to facilitate the frequency determination (see Table 1). The derivative feature resulting from the anomalous dispersion of the water refractive index in this region (Flach et al., 1993a) is fully compensated for in the H_2O system by

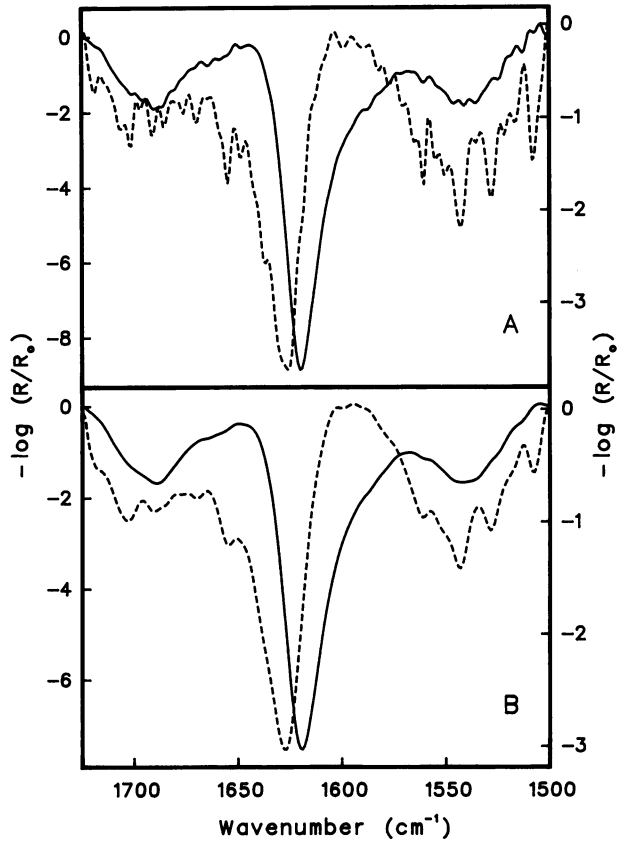

FIGURE 5 The IRRAS of the amide I and II regions for peptide I, a surface active β-sheet peptide, at the A/W (*dashed line*, right-hand ordinate) and air/D_2O (*solid line*, left-hand ordinate) interface before (*A*) and after (*B*) Fourier smoothing using a breakpoint of 0.8. Reflectance absorbance ($-\log(R/R_o)$) is in milliabsorbance units (mAU). Spectra were collected at π = 8 dyne/cm (A/W interface) and at π = 18 dyne/cm (air/D_2O interface). Note: the spectrum for the D_2O subphase is only slightly modified by the smoothing. Water vapor has been subtracted, and the spectra are baseline corrected. 128 scans were coadded.

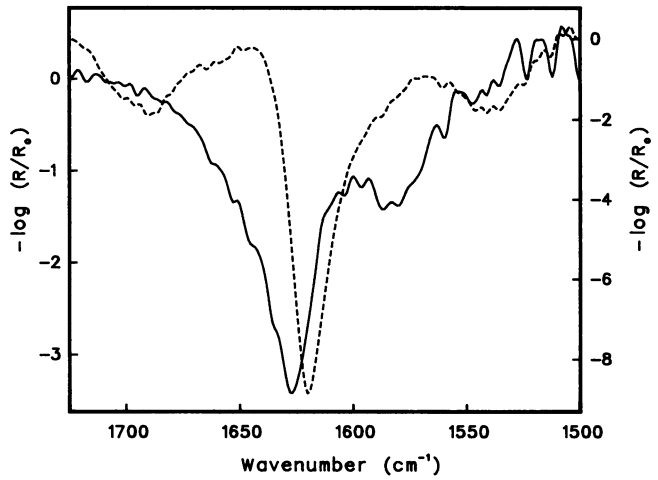

FIGURE 6 The IRRAS of the amide I and II regions for monolayer films of peptide II, a mixed β-sheet/β-turn peptide, (*solid line*, left-hand ordinate) and peptide I, a β-sheet peptide (*dashed line*, right-hand ordinate) on a D_2O subphase. Reflectance absorbance ($-\log(R/R_o)$) is in milliabsorbance units (mAU). The spectrum of peptide II was acquired at π = 13 dyne/cm, and the spectrum of peptide I at π = 18 dyne/cm. Water vapor has been subtracted from the β-sheet peptide only, and both spectra were baseline corrected. 128 scans were coadded.

the trough shuttle modification. An intense amide I band is observed at 1627 cm^{-1} on H_2O along with a weak amide I component at a higher frequency whose shape is distorted by water vapor bands. For the D_2O subphase, frequencies of 1620 and 1689 cm^{-1} are observed for these strong and weak components of the amide I′ band. These observed frequencies are consistent with an antiparallel β-sheet structure (Miyazawa and Blout, 1961). Replacement of H_2O by D_2O in the subphase results in a shift to lower frequency of the amide I band and a decrease in the relative intensity of the amide II to the amide I band, both indicative of HD exchange. Interference in this spectral region from Orn N-trifluoroacetyl groups (absorbance band ~1673 cm^{-1}) in the peptide is negligible (Surewicz et al., 1993).

A comparison of the amide I and II regions in the IRRAS of peptide II (putative β-sheet/β-turn) and peptide I on a D_2O subphase is shown in Fig. 6. The amide I′ band for peptide II is observed at 1627 cm^{-1}, whereas for peptide I the main component occurs at 1620 cm^{-1}. The amide I′ band for peptide II is broadened on the high frequency side, possibly due to a characteristic band associated with turns at ~1665 cm^{-1} (Surewicz and Mantsch, 1988). The presence of the feature at 1580–1585 cm^{-1} (too high in frequency for a residual amide II component) may be due to the aspartic acid asymmetric carboxylate stretch and the symmetric stretch of the deuterium-exchanged guanidino group of arginine residues. The peptide contains 20% of each of these amino acids. Absorbance bands at ~1586 cm^{-1} have been reported for these residues in D_2O solution by transmission IR (Chirgadze et al., 1975). The amide I band of peptide II on an H_2O subphase is observed at 1636 cm^{-1}, 9 cm^{-1} higher than on D_2O (see Table 1). No clear evidence for an isolated higher frequency amide I band was obtained.

SP-C and Peptide III (putative α-helical peptide) at the A/W interface

The amide I and II regions for SP-C, as shown in Fig. 4 *B*, reveal these features at 1654 and 1542 cm^{-1}, respectively, and are characteristic of an α-helical secondary structure, whereas the presence of substantial residual amide II intensity on a D_2O subphase indicates that the peptide group hydrogens are not completely exchanged. These results are completely consistent with previous transmission and ATR FTIR studies of SP-C/phospholipid mixtures (Pastrana et al., 1991). Additional support for a helical structure of this peptide in monolayer form comes from the relative sharpness of the amide I mode, which suggests a regular structure with minimal distortion from idealized geometry, and from the lack of exchange of the peptide bond hydrogen as monitored from the residual amide II intensity, which suggests strong H-bonding.

Fig. 7, *A* and *B* display the amide I and II regions of the IRRAS for peptide III (putative α-helix) at the air/H_2O and

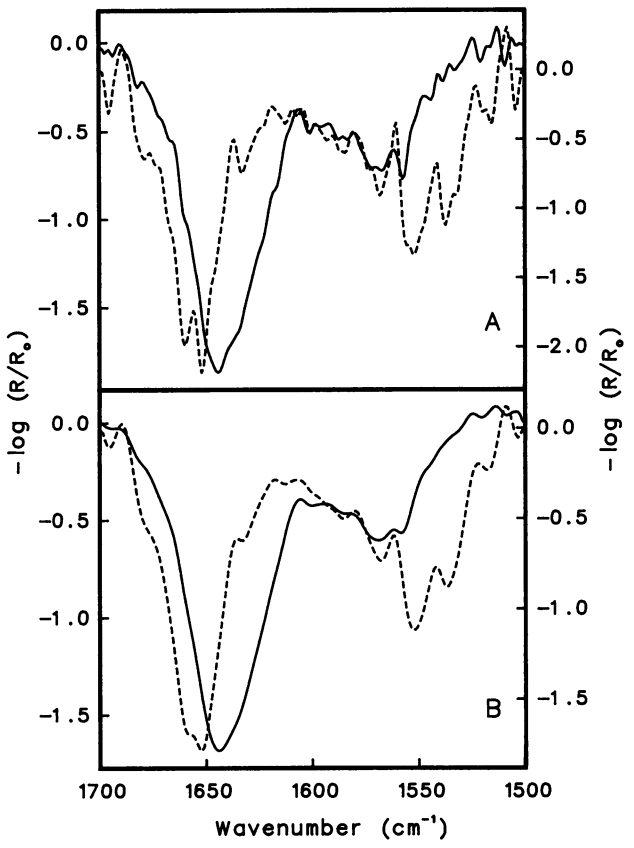

FIGURE 7 The IRRAS of the amide I and II regions for peptide III, an α-helical peptide, at the A/W interface (*dashed line*, right-hand ordinate) and air/D_2O interface (*solid line*, left-hand ordinate) before (*A*) and after (*B*) Fourier smoothing using a breakpoint of 0.8. Reflectance absorbance ($-\log(R/R_o)$) is in milliabsorbance units (mAU). Spectra were collected at $\pi \approx 20$ dyne/cm for an H_2O subphase and at $\pi = 12$ dyne/cm for the D_2O subphase. Water vapor has been subtracted, and the spectra are baseline corrected. 128 scans were coadded.

air/D_2O interfaces before and after smoothing (breakpoint of 0.80), respectively. The observed frequencies are summarized in Table 1. The increased surface area occupied by peptide III compared to peptide I (Taylor, 1990), partially accounts for the decrease in the amide I IRRAS intensity from ~6.8 mAU (peptide I) to ~1.4 mAU (peptide III) for the respective primary amide I′ band on D_2O. Due to the decreased intensity, sharp water vapor bands for both subphases are evident throughout this spectral region and are more pronounced on an H_2O rather than a D_2O subphase. A frequency shift from 1656 to 1645 cm^{-1} and an increase in the halfwidth of the amide I band are observed upon changing the subphase from H_2O to D_2O. The amide II band is virtually absent from peptide spectra acquired from a D_2O subphase, whereas on H_2O this feature is observable at ~1550 cm^{-1}, although it is overlapped by water vapor. The remaining weak band observed on the D_2O subphase at a slightly higher frequency than amide II may be attributed to the asymmetric stretch of the carboxylate group present in the glutamic acid side chains found in this peptide. An IR absorbance band from this residue has been reported at ~1568 cm^{-1} in D_2O solutions (Chirgadze et al., 1975).

The IRRAS evidence for a helical structure for peptide III at the A/W interface is not conclusive. The amide I′ contour is broader then that for SP-C (Fig. 4), and HD exchange leads to a feature in a frequency range appropriate for both α-helical and unordered structures. The amide I and II frequencies (from an H_2O substrate) are indeed appropriate for helical forms, but the overlap with residual water vapor bands affects the accuracy of these frequency measurements. To search for possible solvent-induced conformational changes, CD spectra were obtained for this model helical peptide in H_2O and D_2O solution (data not shown). The spectra indicate that the peptide possesses significant α-helix content in both solutions. Due to lack of sufficient material, quantitative CD analysis could not be undertaken.

Some additional support for the existence of an α-helical conformation at the air/D_2O interface is provided from spectral simulations. The agreement between the theoretically predicted downward shift of the amide I IRRAS band (see Spectral Simulations) versus transmission (both from a D_2O system), and the observed experimental results is encouraging. The simulated spectra are dependent on secondary structure. That is, geometrical parameters required for the simulations assume that the peptide is helical at the interface; the parameters used are similar to those in the caption for Fig. 3. The amide I′ mode for peptide III is observed experimentally at 1646.3 cm^{-1} for a deuterium-exchanged ATR film, and at 1644.7 cm^{-1} for the air/D_2O interface. The input in the simulation for the peak frequency of the absorption band (assumed to have a Lorentzian lineshape) is the same as that observed for the ATR experiment. The observed experimental shift of 1.6 cm^{-1} is reproduced in the simulation of the parallel component on a D_2O subphase. Results from the simulation are also consistent with experimental data from an H_2O subphase. The frequency of the amide I band, observed at 1653 cm^{-1} for an ATR film dried from H_2O solution, is used as the peak position for the latter simulations. The simulations yield a reflectance-absorbance band with a frequency (parallel component) at 1656 cm^{-1}, the same as that observed experimentally.

Peptive IV (putative unordered structure) at the A/W interface

Peptide IV is not very surface active; the π required to produce a spectrum with a detectable amide I band surpasses that of its collapse point. Therefore, it is uncertain whether or not a true monolayer or a collapsed multilayer was sampled. In contrast, the πs at which the IRRAS were acquired for the other peptides were less than that required for film collapse (Taylor, 1990; and unpublished π versus surface area curves).

With the above limitations as a caveat, IRRAS for peptide IV on a D_2O substrate is shown in Fig. 8; the frequency data for both H_2O and D_2O substrates are summarized in Table I. The amide I band frequencies for this peptide, 1655 cm^{-1} (H_2O) and 1642 cm^{-1} (D_2O) are similar to peptide III. The amide II feature (H_2O subphase) occurs at ~1550 cm^{-1} and

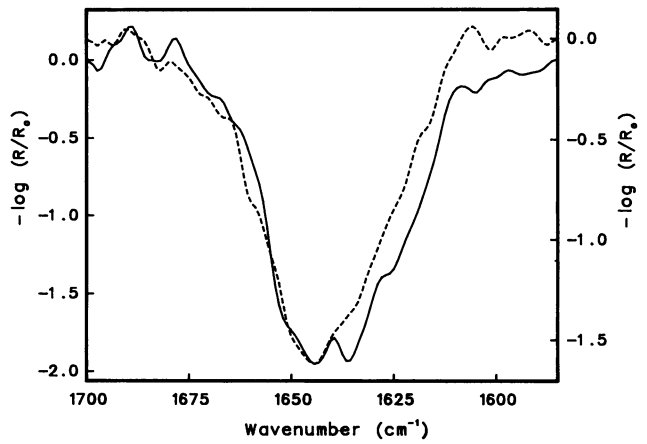

FIGURE 8 The IRRAS of the amide I region for peptide IV, an unordered peptide (*solid line*, left-hand ordinate) and peptide III, a surface active α-helical peptide (*dashed line*, right-hand ordinate) at the air/D_2O interface. Reflectance absorbance ($-\log(R/R_o)$) is in milliabsorbance units (mAU). The spectrum of peptide IV was collected at π = 27 dyne/cm, and the spectrum of peptide III was collected at π = 12 dyne/cm. Water vapor has been subtracted, and the spectra are baseline corrected. 128 scans were coadded.

is again comparable to that observed for the α-helical peptide. Thus, although this peptide was synthesized as a potential unordered structure, the IRRAS evidence is suggestive of a helical form, at least at the πs used.

The amide I′ bands for peptides III and IV are overlaid in Fig. 8. The difference between the two contours is slight; that is, the observed frequencies are both within the range recently reported for exchanged α-helical secondary structure (Tamm and Tatulian, 1993; Frey and Tamm, 1991; Jackson et al., 1991; and Venyaminov and Kalnin, 1990b). In addition, both amide I′ bands are broadened on the low frequency side.

DISCUSSION

The current work provides the first demonstration that reasonable quality spectra may be obtained from protein monolayer films in situ at the A/W interface. Incorporation of the shuttle system into the instrument design reduces the interference from the strong water vapor bands by about an order of magnitude. Residual absorbance of these features is typically $\leq$0.2 mAU. This value permits the characterization of amide I or amide I′ features with absorbance values as small as 1 mAU. Further possible improvements to the device include more accurate temperature control of both the environment and the trough subphase as well as the use of polarized radiation for determination of the orientation of ordered peptide and protein segments.

The spectra-structure correlations serve to emphasize both the strong and weak points in the use of IR spectroscopy for the evaluation of protein and peptide secondary structure. The strong points are best illustrated from the spectra of peptide I (putative β-sheet). In the antiparallel form, this secondary structure is known to produce two characteristic bands in the amide I region, with a strong component in the 1620–1630-cm^{-1} range and a weaker feature near 1680 cm^{-1}. Such a pattern is readily observed (Fig. 5) on the D_2O subphase. The present result therefore identifies the β-sheet as expected, but also shows it to be antiparallel, which was previously unknown and not predictable. Comparison with data from the H_2O subphase reveals a 7–8 cm^{-1} shift for the strong component on deuteration, consistent with previously reported amide I frequencies for deuterium exchanged β-sheet polypeptides (Chirgadze et al., 1973). HD exchange, in this instance, produces no ambiguity in spectra-structure correlations and can be evaluated quantitatively, if necessary, from the residual amide II intensity.

The situation for the putative mixed sheet-turn (peptide II) is complicated by the absence of the characteristic pair of bands expected for the β-sheet element of the suggested structure. It is suggested that the short length of sheet-forming residues produces H-bonding patterns with geometries sufficiently altered from the ideal antiparallel β-sheet structure to eliminate the coupling that produces the splitting in the amide I mode.

The situation for the α-helical modes is more complicated. Spectra for SP-C [known from polarized ATR studies to be predominantly α-helical in a lipidic environment (Pastrana et al., 1991)] show a strong, sharp spectral feature at 1656 cm^{-1} in transmission compared with 1653.6 cm^{-1} in reflection from D_2O. The observed shift is the result of two factors. Spectral distortion from the IRRAS experiment on D_2O shifts the peak by about 1 cm^{-1} to lower frequencies in this system, as discussed in the Spectral Simulations section, whereas partial exchange (judged in this case by the amide I/II intensity ratio on D_2O compared with the ATR spectra) also tends to lower the frequency. The magnitude of this second factor presumably depends on the extent of exchange, the maximum value being about 10–12 cm^{-1} (Venyaminov and Kalnin, 1990b; Jackson et al., 1991; Frey and Tamm, 1991; Trewhella et al., 1989), whereas an 11-cm^{-1} shift was reported for exchanged N-methylacetamide (Miyazawa et al., 1958). The helical amide I feature is relatively sharp, suggestive of a uniform structure.

Peptide III (putative α-helix) is fully exchanged at the A/W interface and produces a spectral shift to 1645 cm^{-1}, as well as a broadened amide I spectral contour. As a result of the 11-cm^{-1} spectral shift, the spectrum of the exchanged peptide strongly resembles that of an unordered form. However, two lines of evidence point to the existence of a helical structure. First, as noted in the results section, the spectral simulations reproduce the observed experimental shifts in the IRRAS experiment. These simulations incorporate helical geometric parameters as input. Second, the bulk- phase secondary structure in D_2O, as judged by CD spectroscopy, is unchanged from H_2O and remains predominantly helical. Despite these suggestive results, a supplementary measurement, such as polarized IRRAS or the observation of vibrational CD in the amide I band (not yet feasible for monolayers in situ, but practical in bulk phases), is required to

absolutely prove the occurrence of α-helical secondary structures at the air/D_2O interface.

To generalize from the current observations, a sharp feature between 1652 and 1658 cm^{-1} is probably safely attributed to an (unexchanged) α-helix. However, if exchange occurs, it is quite likely to produce a shift in those exchanging helical segments to ~1645 cm^{-1}, a region often assumed to arise from unordered conformations. Many recipes for determination of secondary structure from IR amide I data analyze spectra in D_2O environments (Byler and Susi, 1986; Surewicz and Mantsch, 1988; Trewhella et al., 1989; Zhang et al., 1992; and Surewicz et al., 1993). This solvent is chosen to minimize interference from the bending vibration of liquid H_2O near 1640 cm^{-1}. However, this procedure is evidently risky due to the potential shift in the exchanged amide I mode of the α-helix to a frequency overlapped with those of unordered structures. The contributions of side-chain modes to the amide I contour must also be considered. The position of maximum frequency for these bands can be dependent on solvent, pH, and/or pD (Chirgadze et al., 1975; Venyaminov and Kalnin, 1990a).

The current apparatus permits the direct investigation of protein secondary structures (with the limitations noted above) at the A/W interface. Studies currently in progress incorporating polarized radiation will remove the ambiguities and permit the helix and random coil structures to be distinguished. In addition to secondary structure information from proteins, previous work has shown that acyl-chain conformation and head-group ion binding may be determined in phospholipid monolayers (Hunt et al., 1989; Flach et al., 1993b). Thus, a relatively complete molecular characterization of experimental paradigms (monolayers) that provide excellent models for pulmonary surfactant and peptide interaction with phospholipids is now available. Several applications of this technology are in progress.

This work was supported by the Public Health Service (Grant GM-29864 to R.M.). Funds for the spectrometer construction were provided by Rutgers University.

REFERENCES

Barany, G., and R. B. Merrifield. 1979. Solid-phase peptide synthesis. *In* The Peptides, (Gross, E., and Meienhofer, J., eds.) Vol. 2, pp. 3:254, Academic Press, London.

Becker, R. 1964. *Electromagnetic Fields and Interactions. Volume II. Quantum Theory of Atoms and Radiation.* Blaisdell Publishing Co., New York.

Böhm, C., H. Möhwald, L. Leiserowitz, J. Als-Nielsen, and K. Kjær. 1993. Influence of chirality on the structure of phospholipid monolayers. *Biophys. J.* 64:553–559.

Boyle III, J., and A. J. Mautone. 1982. A new surface balance for dynamic surface tension studies. *Colloids Surf.* 4:77–85.

Byler, D. M., and H. Susi. 1986. Examination of the secondary structure of proteins by deconvolved FTIR spectra. *Biopolymers.* 25:469–487.

Chirgadze, Y. N., O. V. Fedorov, and N. P. Trushina. 1975. Estimation of amino acid residue side-chain absorption in the infrared spectra of protein solutions in heavy water. *Biopolymers.* 14:679–694.

Chirgadze, Y. N., B. V. Shestopalov, and S. Y. Venyaminov. 1973. Intensities and other spectral parameters of infrared amide bands of polypeptides in the β- and random forms. *Biopolymers.* 12:1337–1351.

Cornell, D. G. 1978. Circular dichroism of polypeptide monolayers. *J. Colloid Interface Sci.* 70:167–180.

DeGrado, W. F., and J. D. Lear. 1985. Induction of peptide conformation at apolar/water interfaces. 1. A study with model peptides of defined hydrophobic periodicity. *J. Amer. Chem. Soc.* 107:7684–7689.

Dluhy, R. A. 1986. Quantitative external reflection infrared spectroscopic analysis of insoluble monolayers spread at the air-water interface. *J. Phys. Chem.* 90:1373–1379.

Dluhy, R. A., M. L. Mitchell, T. Pettenski, and J. Beers. 1988. Design and interfacing of an automated Langmuir-type film balance to an FT-IR spectrometer. *Appl. Spectrosc.* 42:1289- 1293.

Dluhy, R. A., K. E. Reilly, R. D. Hunt, M. L. Mitchell, A. J. Mautone, and R. Mendelsohn. 1989. Infrared spectroscopic investigations of pulmonary surfactant-surface film transitions at the air-water interface and bulk phase thermotropism. *Biophys. J.* 56:1173–1181.

Downing, H. D., and D. Williams. 1975. Optical constants of water in the infrared. *J. Geophys. Res.* 80:1656–1661.

Flach, C. R., J. W. Brauner, and R. Mendelsohn. 1993a. Coupled external reflectance FT-IR/miniaturized surface film apparatus for biophysical studies. *Appl. Spectrosc.* 47:982- 985.

Flach, C. R., J. W. Brauner, and R. Mendelsohn. 1993b. Calcium ion interactions with insoluble phospholipid monolayer films at the A/W interface. External reflection-absorption IR studies. *Biophys. J.* 65: 1994–2001.

Fraser, R. D. B., and T. P. MacRae. 1973. *Conformation in Fibrous Proteins and Related Synthetic Peptides.* Academic press, New York.

Frey, S., and L. K. Tamm. 1991. Orientation of melittin in phospholipid bilayers. A polarized attenuated total reflection infrared study. *Biophys. J.* 60:922–930.

Fukushima, D., J. P. Kupferberg, S. Yokoyama, D. J. Kroon, E. T. Kaiser, and F. J. Kedzy. 1979. A synthetic amphiphilic helical docosapeptide with the surface properties of plasma apolipoprotein A-I. *J. Am. Chem. Soc.* 101:3703–3704.

Helm, C. A., P. Tippmann-Krayer, H. Möhwald, J. Als-Nielsen, and K. Kjær. 1991. Phases of phosphatidyl ethanolamine monolayers studied by synchrotron x-ray scattering. *Biophys. J.* 60:1457–1476.

Hunt, R. D., M. L. Mitchell, and R. A. Dluhy. 1989. The interfacial structure of phospholipid monolayer films: an infrared reflectance study. *J. Mol. Struct.* 214:93–109.

Jackson, M., P. I. Haris, and D. Chapman. 1991. Fourier transform infrared spectroscopic studies of Ca^{2+}-binding proteins. *Biochemistry.* 30:9681–9686.

McConnell, H. M., L. K. Tamm, and R. M. Weis. 1984. Periodic structures in lipid monolayer phase transitions. *Proc. Natl. Acad. Sci. USA.* 81: 3249–3253.

McIntyre, J. D. E. 1973. Specular reflection spectroscopy of the electrode-solution interphase. *In* Advances in Electrochemistry and Electrochemical Engineering. Vol. 9. R. H. Muller, editor. Wiley-Interscience, New York. 61–166.

Mitchell, M. L., and R. A. Dluhy. 1988. In situ FT-IR investigation of phospholipid monolayer phase transitions at the air-water interface. *J. Amer. Chem. Soc.* 110:712–718.

Miyazawa, T., and E. R. Blout. 1961. The infrared spectra of polypeptides in various conformations: Amide I and II bands. *J. Amer. Chem. Soc.* 83:712–719.

Miyazawa, T., Y. Shimanouchi, and S. Mizushima. 1958. Normal vibrations of N-methylacetamide. *J. Chem. Phys.* 29:611–616.

Möhwald, H. 1990. Phospholipid and phospholipid-protein monolayers at the air/water interface. *Annu. Rev. Phys. Chem.* 41:441–476.

Ösapay, G., and J. W. Taylor. 1992. Multicyclic polypetide model compounds. 2. Synthesis and conformational properties of a highly α-helical uncosapeptide constrained by three side-chain to side-chain lactam bridges. *J. Amer. Chem. Soc.* 114:6966–6973.

Osterman, D. G., and E. T. Kaiser. 1985. Design and characterization of peptides with amphiphilic β-strand structures. *J. Cell. Biochem.* 29:57–72.

Pastrana, B., A. J. Mautone, and R. Mendelsohn. 1991. Fourier transform infrared studies of secondary structure and orientation of pulmonary surfactant SP-C and its effect on the dynamic surface properties of phospholipids. *Biochemistry.* 30:10058–10064.

Pastrana-Rios, B., C. R. Flach, J. W. Brauner, A. J. Mautone, and R. Mendelsohn. 1994. A direct test of the "squeeze-out" hypothesis of lung

surfactant function. External reflection FT-IR at the air/water interface. *Biochemistry.* 33:5121–5127.

Peters, R., and K. Beck. 1983. Translational diffusion in phospholipid monolayers measured by fluorescence microphotolysis. *Proc. Natl. Acad. Sci. USA.* 80:7183–7187.

Surewicz, W. K., and H. H. Mantsch. 1988. New insight into protein secondary structure from resolution-enhanced infrared spectra. *Biochim. Biophys. Acta.* 952:115–130.

Surewicz, W. K., H. H. Mantsch, and D. Chapman. 1993. Determination of protein secondary structure by Fourier Transform infrared spectroscopy: A critical assessment. *Biochemistry.* 32:389–394.

Tamm, L. K., and S. A. Tatulian. 1993. Orientation of functional and nonfunctional PTS permease signal sequences in lipid bilayers. A polarized attenuated total reflection infrared study. *Biochemistry.* 32: 7720–7726.

Taylor, J. W. 1990. Peptide models of dynorphin A(1–17) incorporating minimally homologous substitutes for the potential amphiphilic β-strand in residues 7:15. *Biochemistry.* 29:5364–5373.

Trewhella, J., W. K. Liddle, D. B. Heidorn, and N. Strynadka. 1989. Calmodulin and troponin C structures studied by Fourier Transform infrared spectroscopy: Effects of Ca^{2+} and Mg^{2+} binding. *Biochemistry.* 28: 1294–1301.

Venyaminov, S. Y., and N. N. Kalnin. 1990a. Quantitative IR spectrophotometry of peptide compounds in water (H_2O) solutions. I. Spectral parameters of amino acid residue absorption bands. *Biopolymers.* 30: 1243–1257.

Venyaminov, S. Y., and N. N. Kalnin. 1990b. Quantitative IR spectrophotometry of peptide compounds in water (H_2O) solutions. II. Amide absorption bands of polypeptides and fibrous proteins in α-, β-, and random coil conformations. *Biopolymers.* 30:1259–1271.

von Tscharner, V., and H. M. McConnell. 1981. An alternative view of phospholipid phase behavior at the air-water interface. *Biophys. J.* 36:409–419.

Zhang, Y., R. N. A. H. Lewis, R. S. Hodges, and R. N. McElhaney. 1992. FTIR spectroscopic studies of the conformation and amide hydrogen exchange of a peptide model of the hydrophobic transmembrane α-helices of membrane proteins. *Biochemistry.* 31:11572–11578.